Numerical Simulations of Energy Transfer in Interacting Counter-streaming Plasmas

S. P. Davis[1], V. Tikhonchuk[1], E. d'Humières[1]

A. V. Brantov[1,2]

S. Bochkarev[1,2]

R. Capdessus[1]

I. Andriyash

S. Jequier[1]

1. University Bordeaux 1, France
CELIA – CEA – CNRS

2. P.N. Lebedev Physics Institute, Russian Academy of Sciences, Moscow, Russias

davis@celia.u-bordeaux1.fr

Omega Laser Facility Users Group Workshop: 25 April–27 April | Rochester, NY

Support

United States of America Department of Defense: Army Research Laboratory. RDECOM-CERDEC/ITC-A

United States of America Department of State: Fulbright Scholarship Program

Outline

Introduction, Motivations: Project began as Fulbright Scholarship: Laboratory Astrophysics with Observational considerations

Project: TNSA Mechanism. Model, at lab scale, energy exchange in counter-streaming plasmas leading to collisisonless shocks: TNSA Accelerated ions interact with secondary plasma jet target

- **Focus: Spatial analysis in the overlapping interaction region.**
- **Energy / Particle Density, Fields, One Filament**
- **Quantify role of electron heating with instabilities**

Methods: PIC simulations [Sentoku, Y. & Kemp A. J., 2008, J. Comp. Phys. 227]; MANDOR [D. V. Romanov et al., Phys. Rev. Lett. 93]

- **Optimization. 2D: PICLS. 3D: MANDOR**
- **Astrophysics Connection**
- **Results, Summary and Conclusions**

Motivations

- **Here: using astrophysical parameters, evaluate : electron heating w/ instabilities for energy transfer in counter-streaming plasmas (Davis et al, ApJ, 2012: in preparation; Davis et al. IOP, 244 (2010))**
- **TNSA: laser accelerated, Energetic protons at sub-relativistic velocities. Overdense targets.**

***Previous Work*:**

Theoretical: Kato & Takabe arXiv:1003.1217v1 (2010): e.s. i—i instability occurs in front of shock and so does Weibel w/ B-field. ; Kato & Takabe ApJ, 681, 2008: Weibel mediated shocks may ocurr at low velocity; Y. Lyubarsky & D. Eichler, ApJ, 647, 2006: a fraction ε_B ~ 10^{-4} of the total energy is converted into magnetic energy unless the electrons are heated greatly in the shock

Experimental: Ross et al., POP 19, 2012: Omega: high velocity counter-streaming plasma flows for collisionless shocks. Kuramitsu, Y. et al., PRL 106, (2011): electrostatic collisionless shock formation in very-high-velocity counterstreaming plasmas. Weibel filaments not seen – need much larger laser energy for Weibel-mediated shock.

CH-H^+ Foil Target Normal Sheath Acceleration

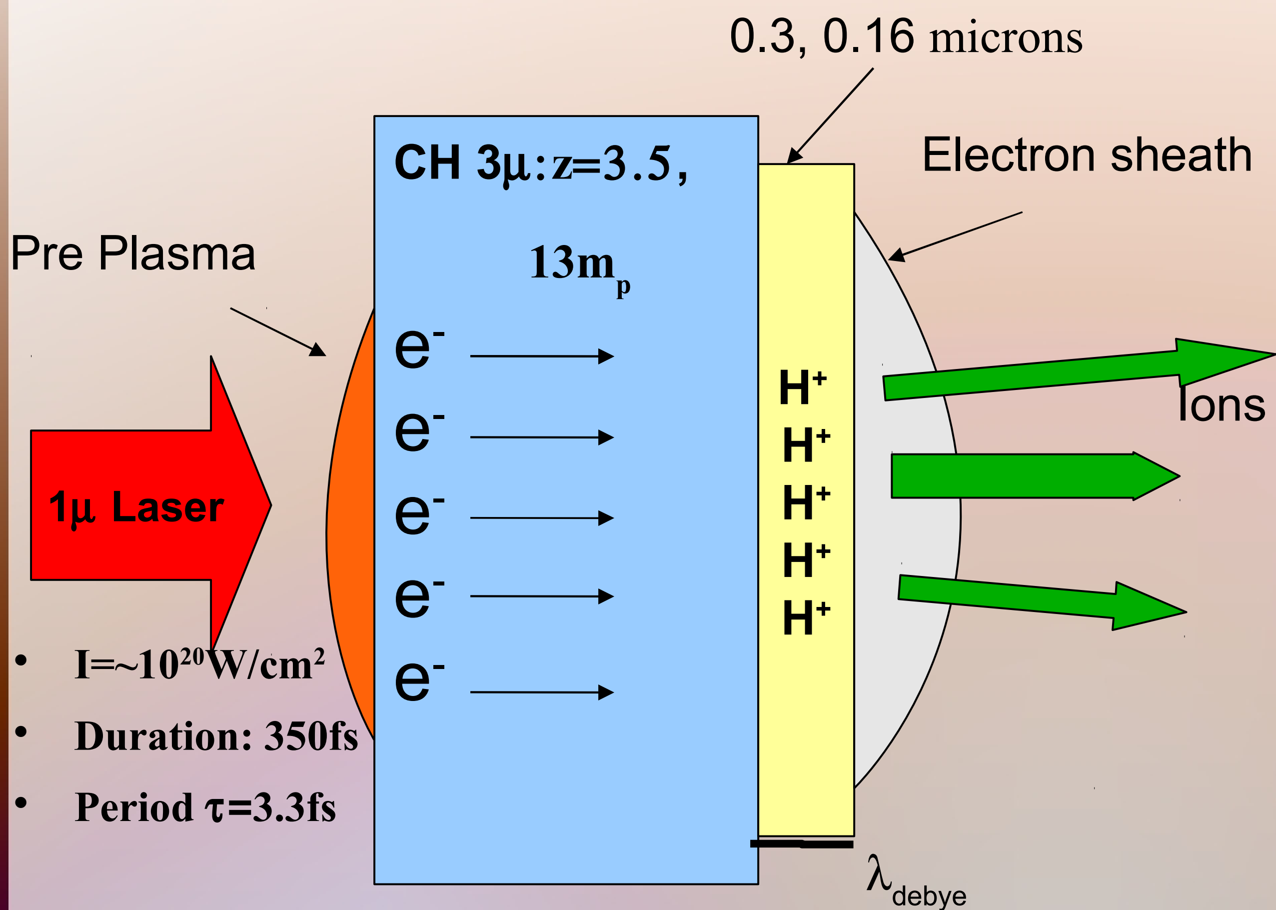

III. Target Normal Sheath Acceleration

$E_i \sim 10 \times T_e$

- **Electrons penetrate target & form dense sheath on rear, non-irradiated surface**
- **Strong electrostatic sheath field ionizes surface layer ($E_o \sim kT / e\lambda_d \sim$ MV/μm)**
- **Rapid (~ps) acceleration in expanding sheath produces very nearly laminar ion beam**

- **Parameters represent LULI (Laboratoire pour l'Utilisation des Lasers Intenses)**
- **Extract a proton bunch by separating them from heavier carbon in CH Foil**
- **Laser pulse can be at oblique incidence (Snavely R A et al 2000, Phys. Rev. Lett. 85 2945; Fuchs J et al . 2005, PRL. Lett. 94; Fuchs J et al 2009, C. R. Phys. 10; Passoni, M., Bertagna, L., Zani, A.2010 New J. Phys. 12)**

Optimization: Dependency on Laser and Target Parameters: Set-up

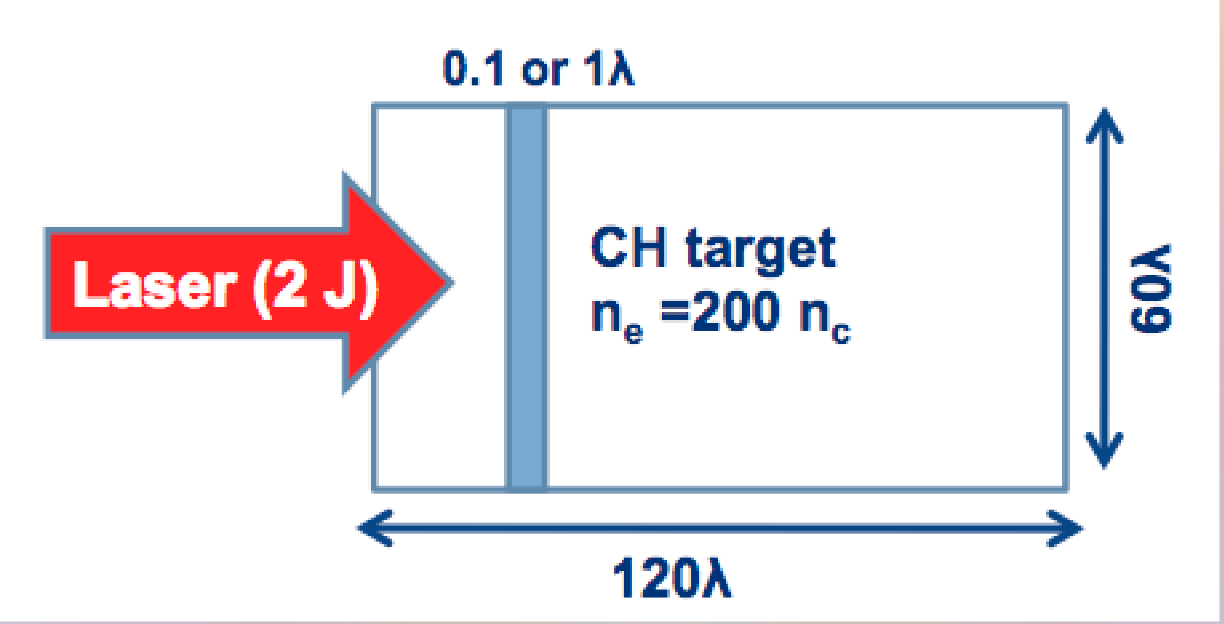

Setup of the first 2D optimization study. Concentration ratio for CH is 4 protons for each carbon ion and electrons with a constant density at 200 n_c. (E. d’Humières, et al., 2011, in preparation)

Maximum proton energy for various laser, target parameters: 2D optimization with PICLS (p-polarization)

	Intensity ($x10^{18}$ W/cm^2)	Laser pulse duration (fs)	Laser FWHM (μm)	Maximum proton energy (max, MeV)
0.1 μm target	100	45	6	25.5
	50	90	6	25.2
	225	20	6	15.9
	40	45	10	15.9
	225	45	4	**36.9**
1 μm target	100	45	6	9
	50	90	6	15.9
	225	20	6	3
	40	45	10	4.5
	225	45	4	15.3

Optimization results: 2D, 3D via MANDOR - optimum laser parameters from PICLS. $I_{Laser} = 2.25\times10^{20}$ W/cm^2, pulse duration = 45 fs and FWHM = 4 λ. Optimum thickness = 0.4 λ. Maximum E_{proton} = 53 MeV in the 2D case and 38 MeV in the 3D case. 2D simulations overestimate 1.5–2 times proton energy compared to 3D simulations.
(E. d'Humières, et al., 2011, in preparation)

Optimum number of protons for 10-30 MeV regime: 4.25×10^{10} protons for the 20 J/50 fs laser pulse, we need at least 10^{13} protons → kJ/ps pulse

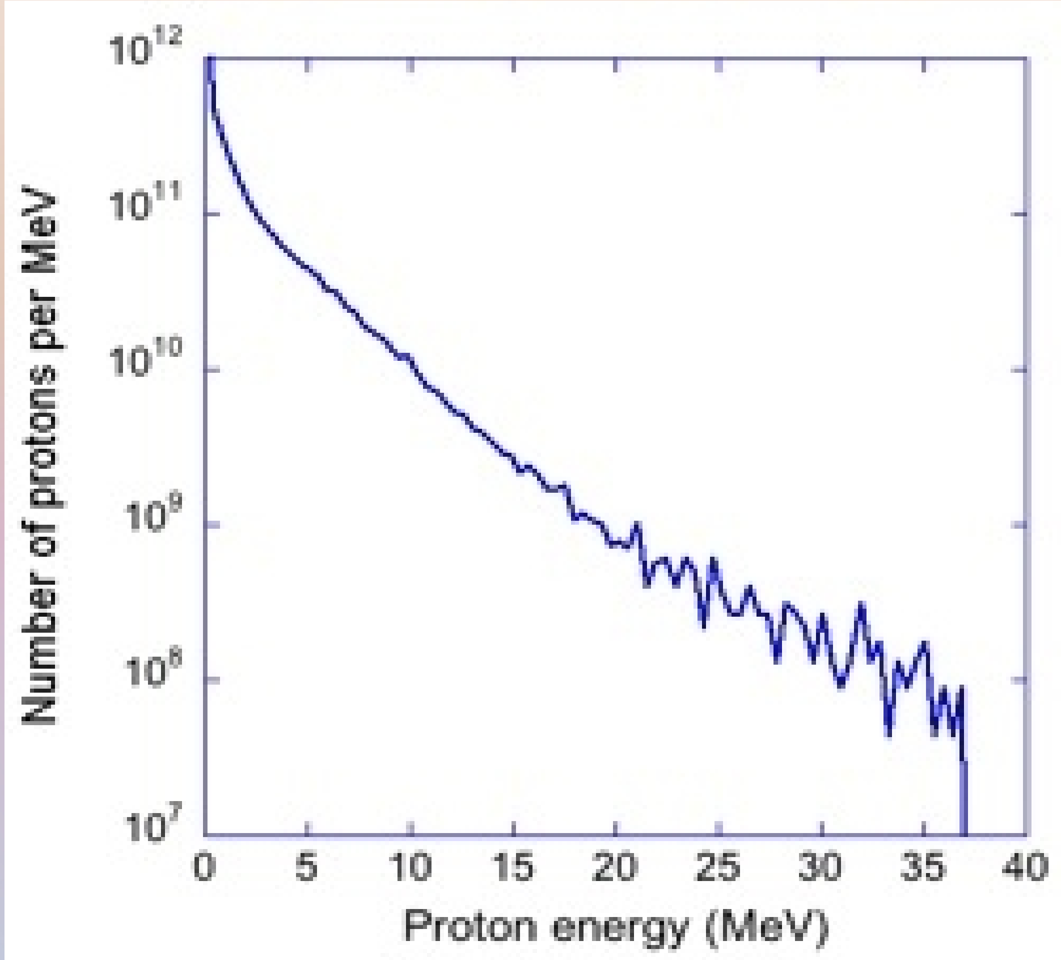

The corresponding spectrum in protons per MeV

Counter-Streaming Plasmas Interaction via LPI

- Our Experimental Scheme:
  - interaction w/ secondary plasma jet target => instabilities within the overlap region
- Ion bunches: provide directed kinetic energy collisionless transfer from protons to electrons, to magnetic and electric fields
- Demonstrate: Ion Weibel produces energy exchange [Davis et al., 2010 J. Phys.: Conf. Ser. 244]; Davis et al 2012: European Journal Web of Conf., submitted
- Energy Equipartition: ions => electrons => fields

Interaction Simulation Box: PIC parameters with Astrophysical Considerations

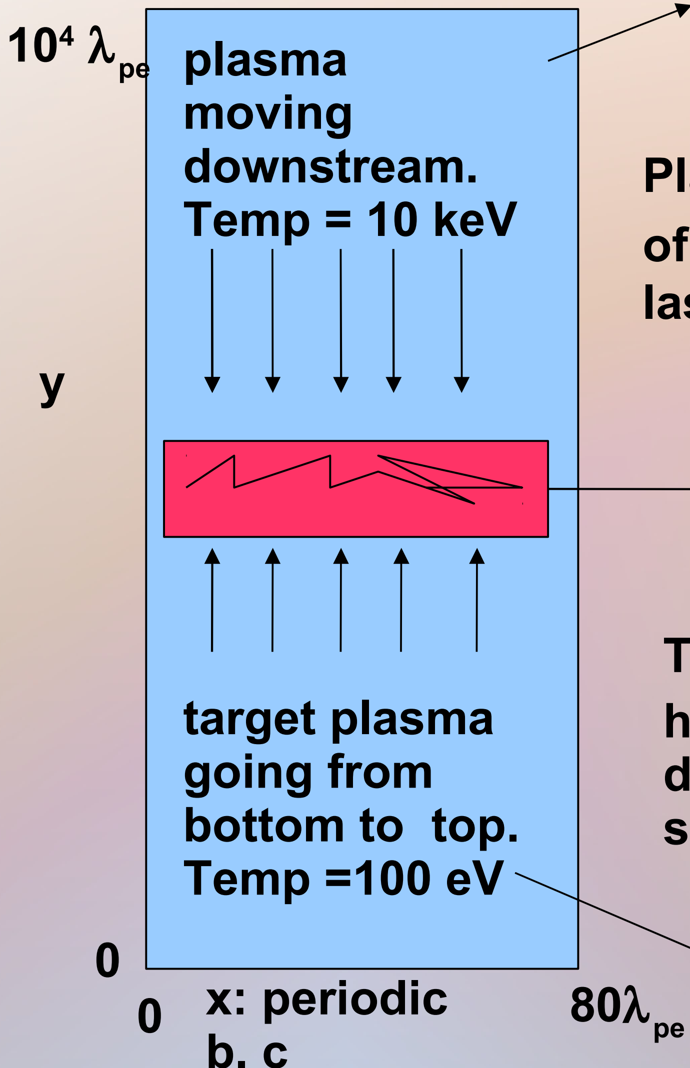

Represents External jet with realistic mass ratio, from, e.g, a GRB

Plasmas: equal density $n_e = 10^{18}$ particles (<=> # of protons accelerated to ~ 20MeV with a ps kJ laser pulse), equal bulk velocity = v_p = 0.2c

Overlap region where counter streaming plasmas interact

The ion inertia length is $2\pi c/\omega_{pi} = 42.8\lambda_{pe}$, half the simulation box in the transverse direction, but > 200 times smaller than the simulation box in the propagation direction.

Represents ISM. jet+ISM= afterglow, for GRB case

$\lambda_{pe} = 2\pi c/\omega_{pe}$ = electron skin depth = 33.4 microns for this density

λ_0 = 1 for this presentation

GRB Image with Afterglow
*Beppo*SAX X-Ray Satellite

GRB970228

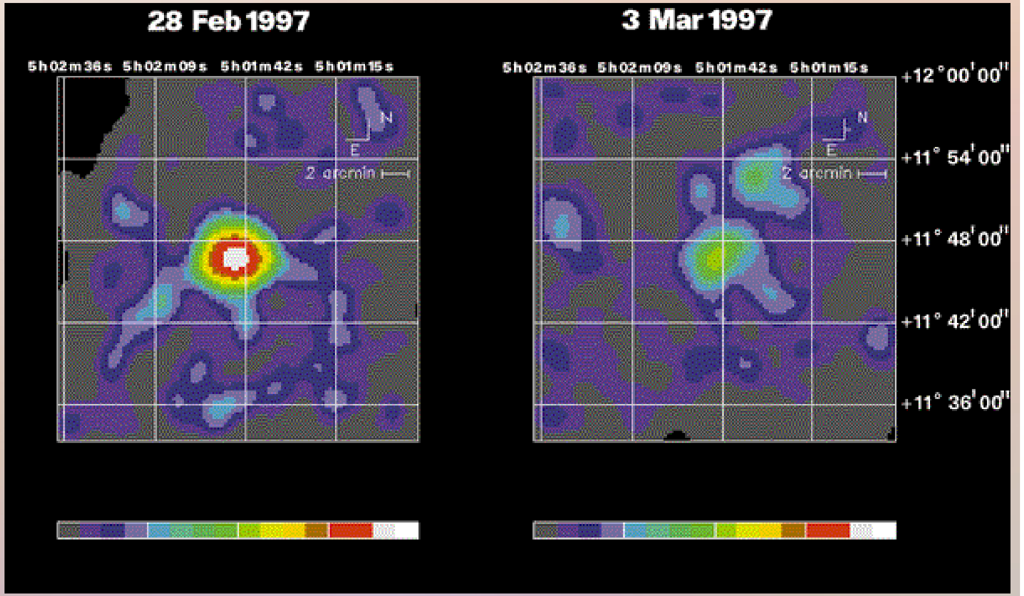

GRB970228 location procedure

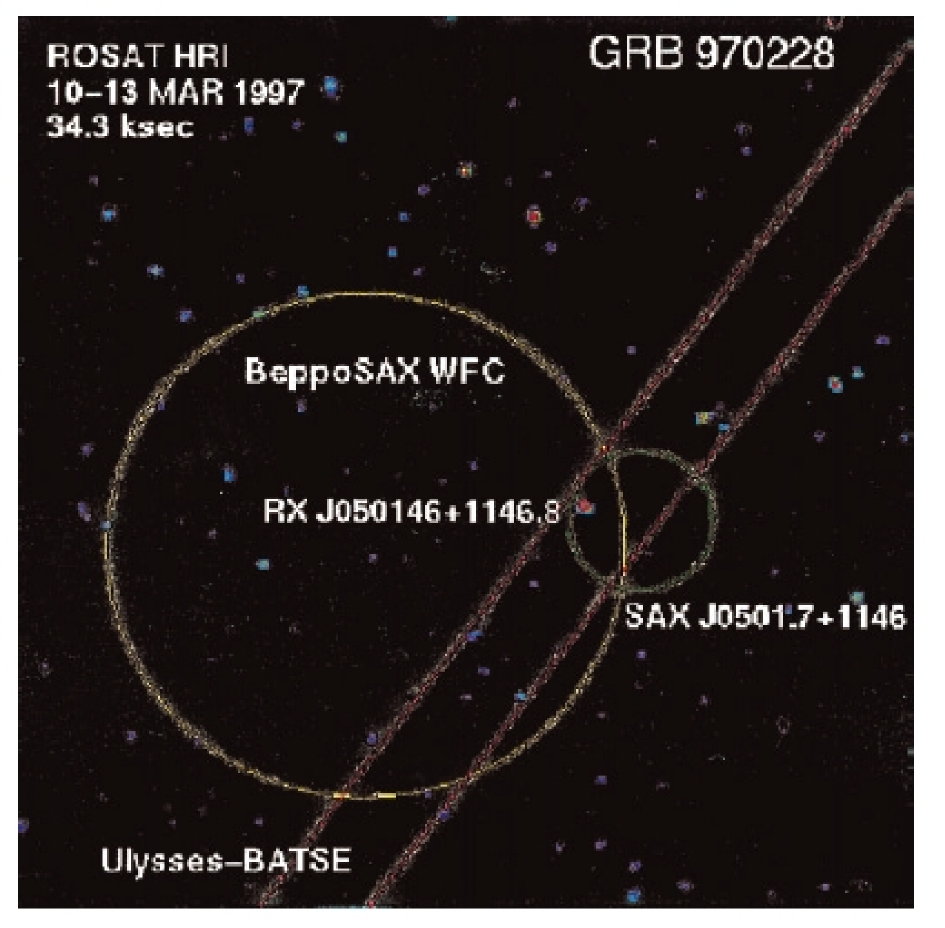

Costa, Frontera, Heise et al., Nature, 1997, GRB970228
Frontera, Costa, Piro et al., ApJL 1998. Jets: see Piran, ApJ, 519:L17-L20, 1999; Piran, REV. OF MOD. PHY., 76, 2004

Frontera et al. , A&A, 2008

PICLS Parameters Summary of interaction: colliding counter streaming plasmas. Based on astrophysical observations (Davis et al, ApJ, 2011, in preparation)

Simulations conducted in center of mass frame

- Simulation Box Geometry: 80 in transverse direction (x) and 10^4 in propagation direction (y), units of $\lambda_{pe} = 2\pi c/\omega_{pe}$ = electron skin depth = 33.4 microns for this density.

- Results: can be rescaled to any other density, by having λ_{pe} and $T_{pe} = 2\pi/\omega_{pe}$ 0.11 ps as the spatial and temporal scales

- Very long box provides for a long time simulation: necessary for appropriate assessment of ion energy losses
  - Observed filaments are from the Weibel instability, it develops faster from the bottom: the electrons have a lower temperature

Global Properties: Temporal Evolution of Electron Energy Density for simulation time $\tau = \omega_{pi}t$ = 10, 20, 30, 40 (400, 800, 1200, 1600 pp)

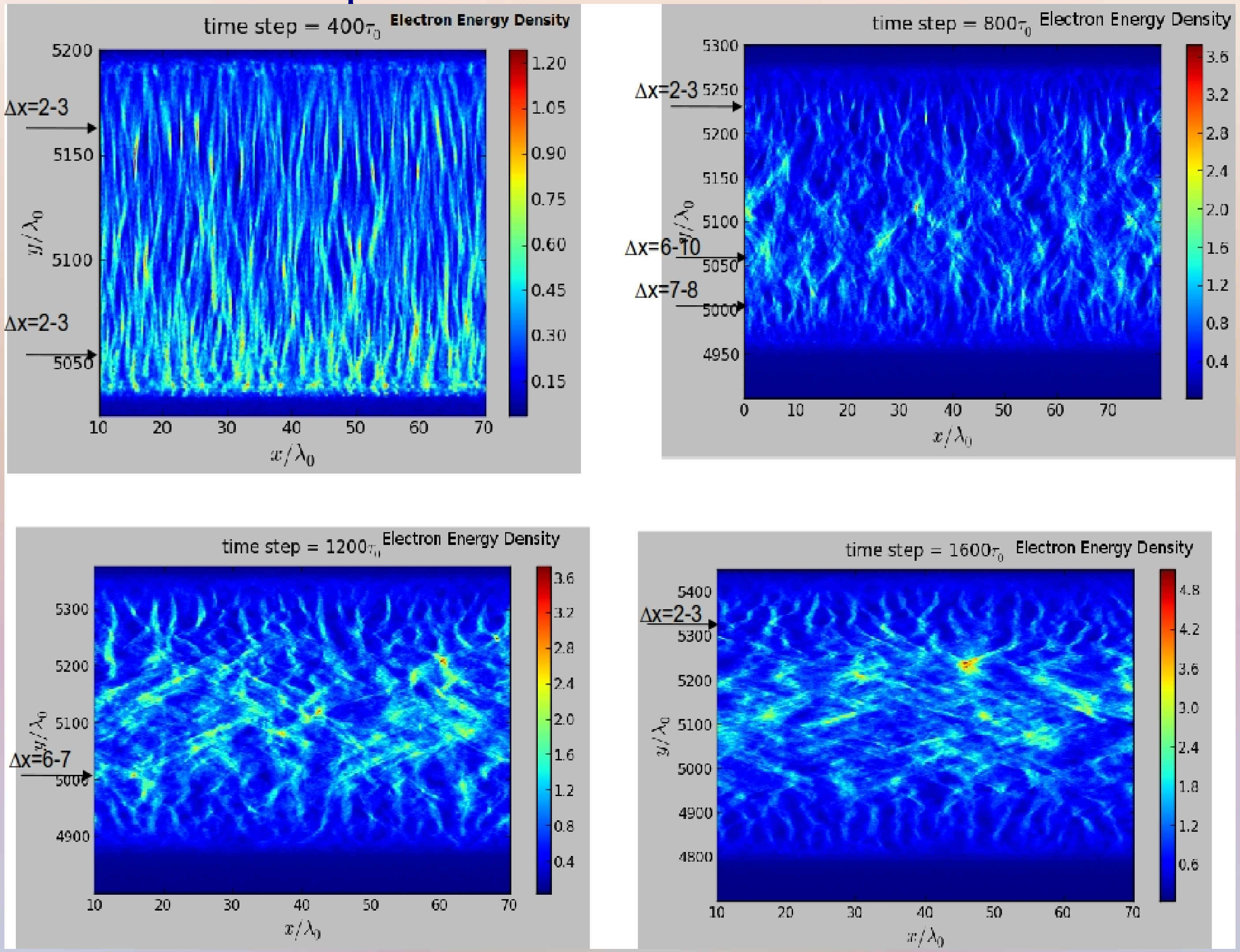

$\lambda_0 = 1$

Peak to peak separation is changes over time as filaments appear and then merge: filaments have energy density enhanced zones or hot spots.

Electron Energy Density. Filament Row. 400plasma periods: simulation time 10. Behavior within a single snapshot

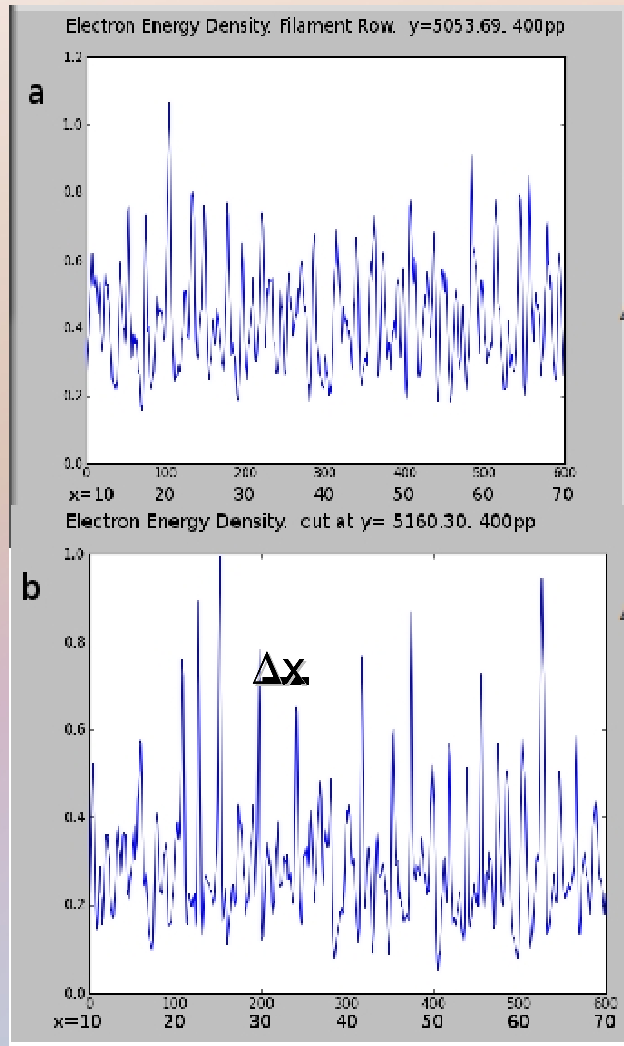

Peak to peak separation remains the same for this time

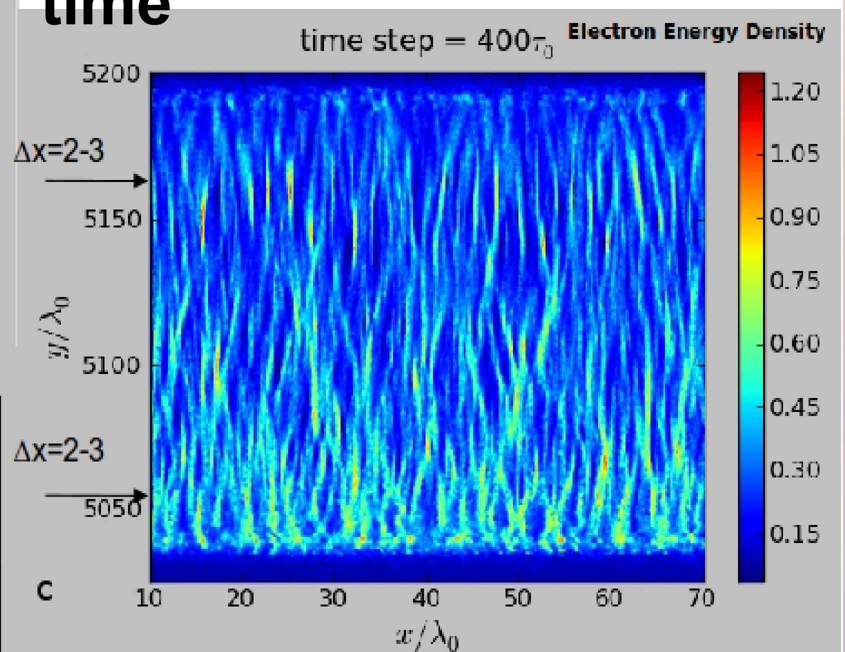

Filament length is of the order of 100 ion inertial lengths

Early onset of Weibel instability produces electron density modulation in the direction perpendicular to the streaming axis with the period of the order of 2~3 electron inertia length.

Electron Energy Density. Filament Row. 800 plasma periods: simulation time 20. Behavior within a single snapshot

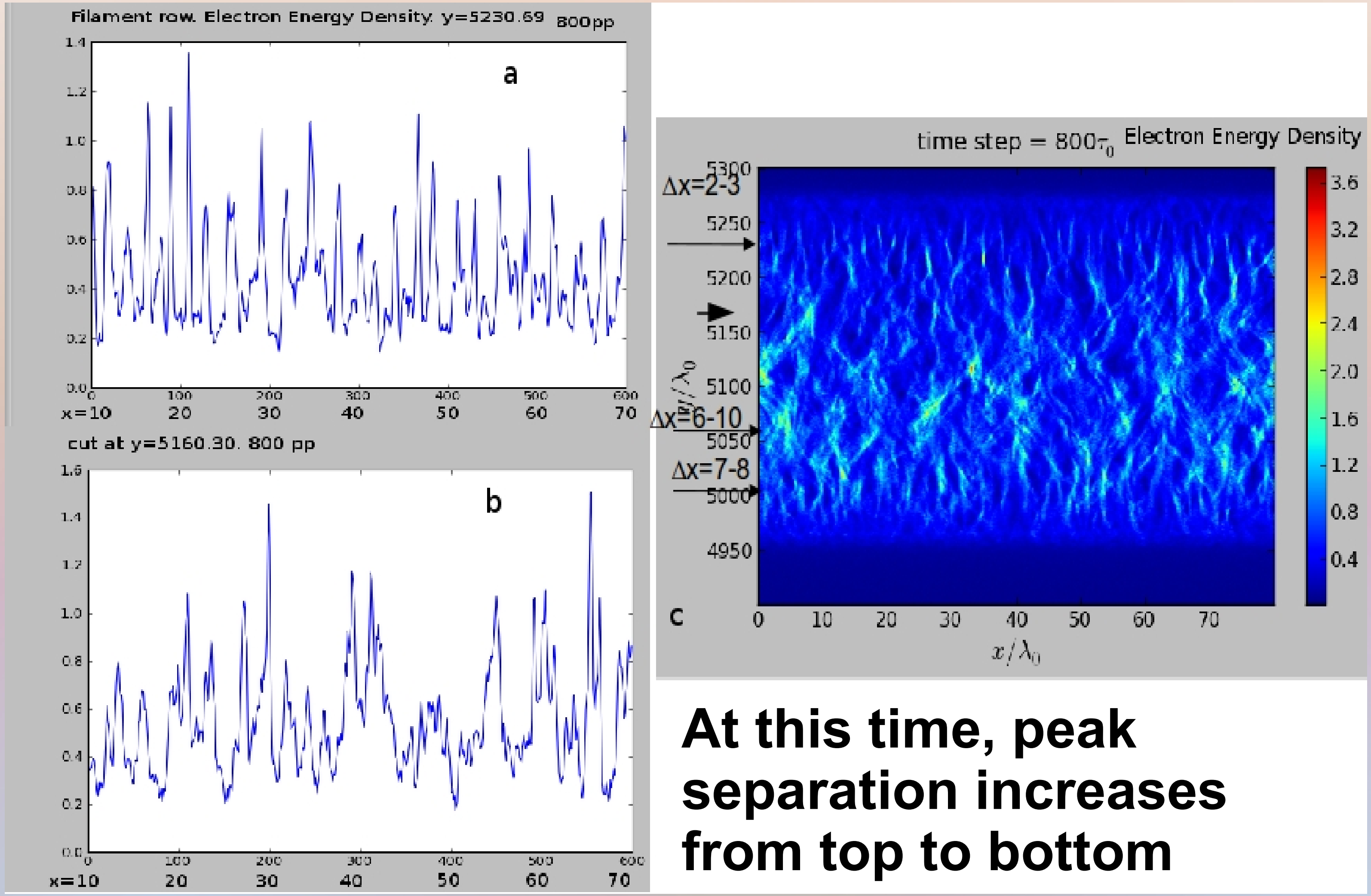

At this time, peak separation increases from top to bottom

Global Properties: Temporal Evolution of Ion Energy Density for simulation times 10, 20, 30, 40

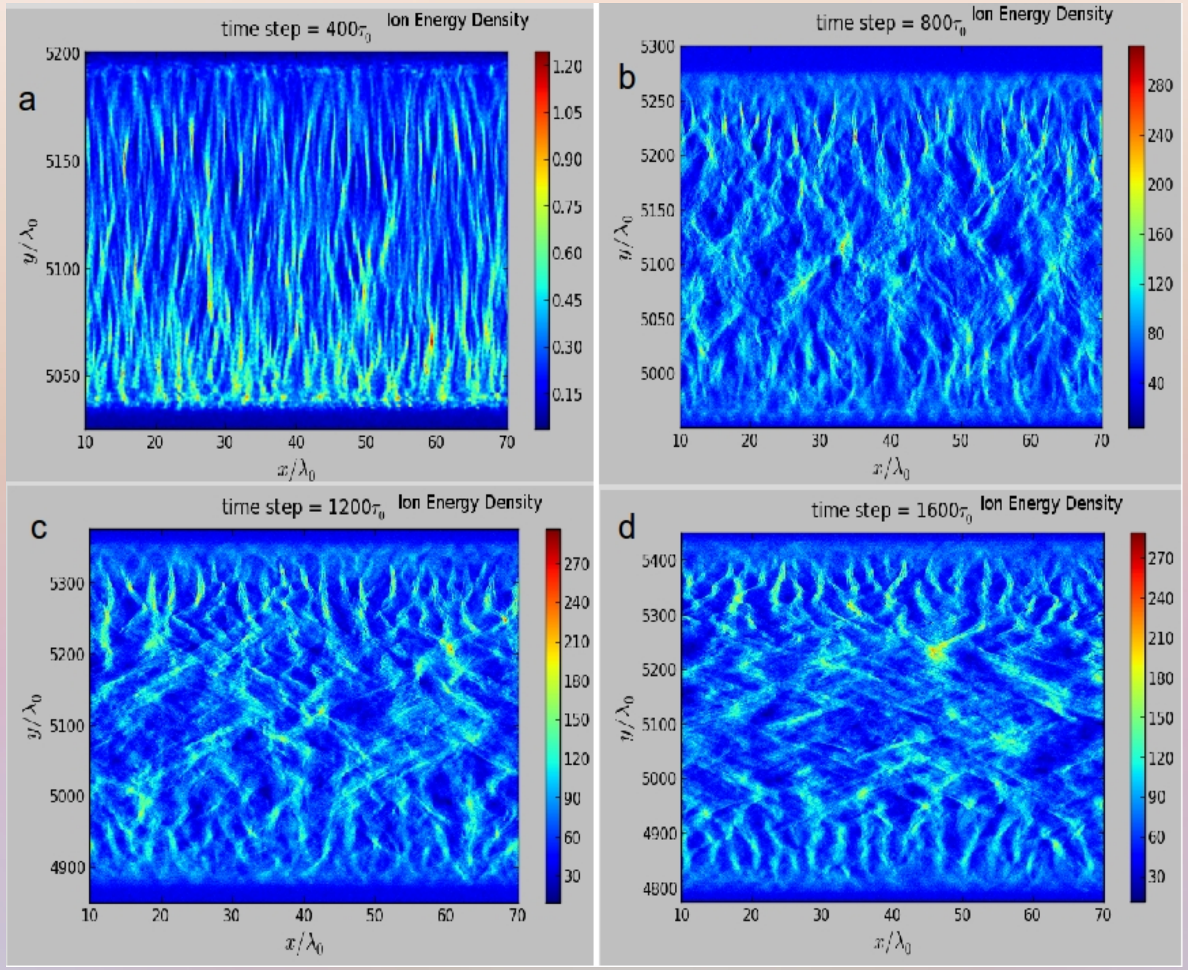

Ion filamantation occurs on the electron spatial scale. Hence, it is electron driven - a consequence of the electron Weibel instability

Magnetic Field z--Component Temporal Evolution for simulation times 10, 20, 30 and 40

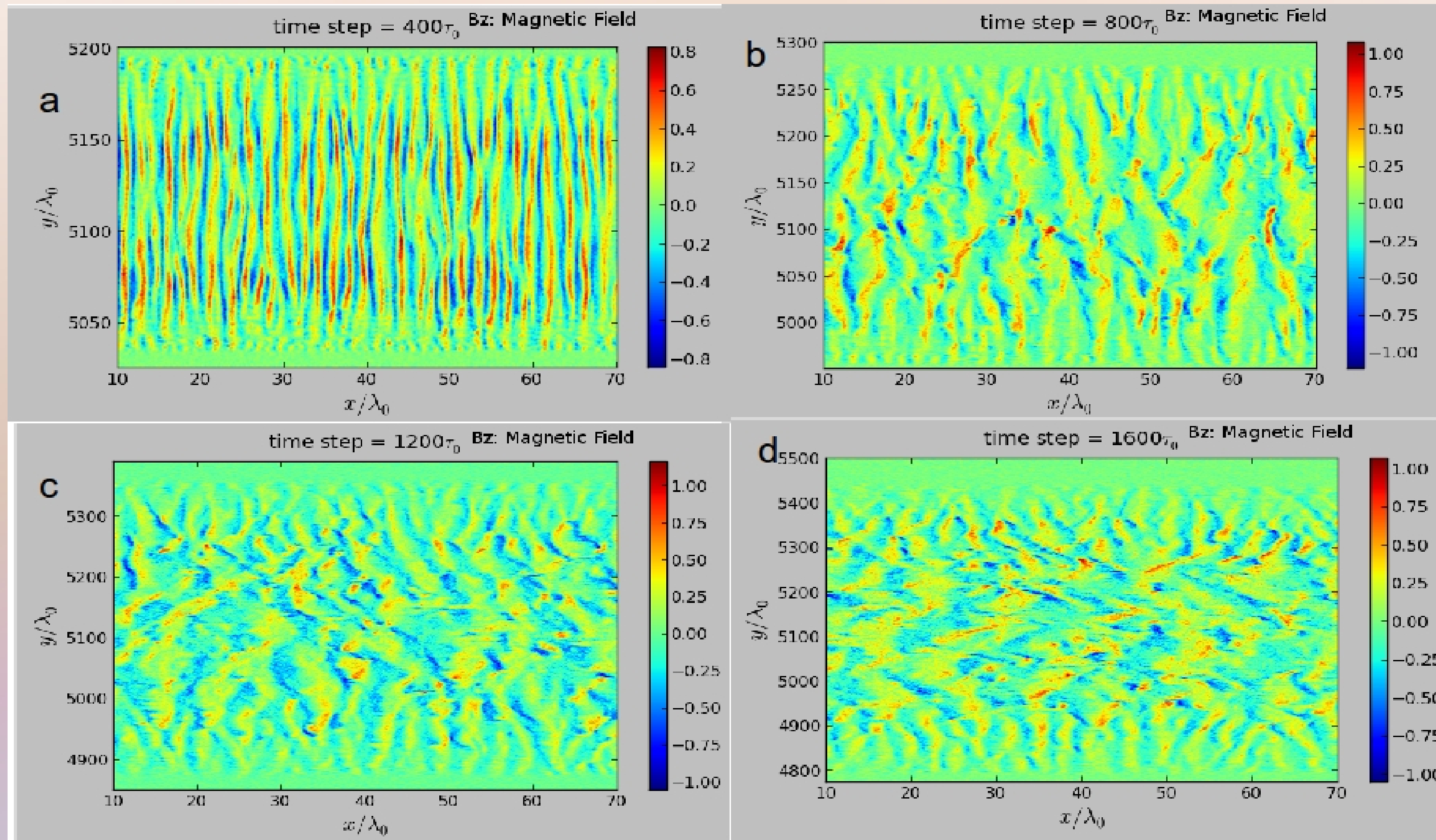

Early on, Weiblel – like filaments occur and then break up and disperse. B~ $0.8m_e\omega_{pe}/e$; current j~$0.4en_0c$. The magnetic field is the result of the Weibel instability. Filament scales, position: correlate with density, energy

Bz filament row with Bz magnetic field for three simulation snapshots at simulation times 20, 30 and 40

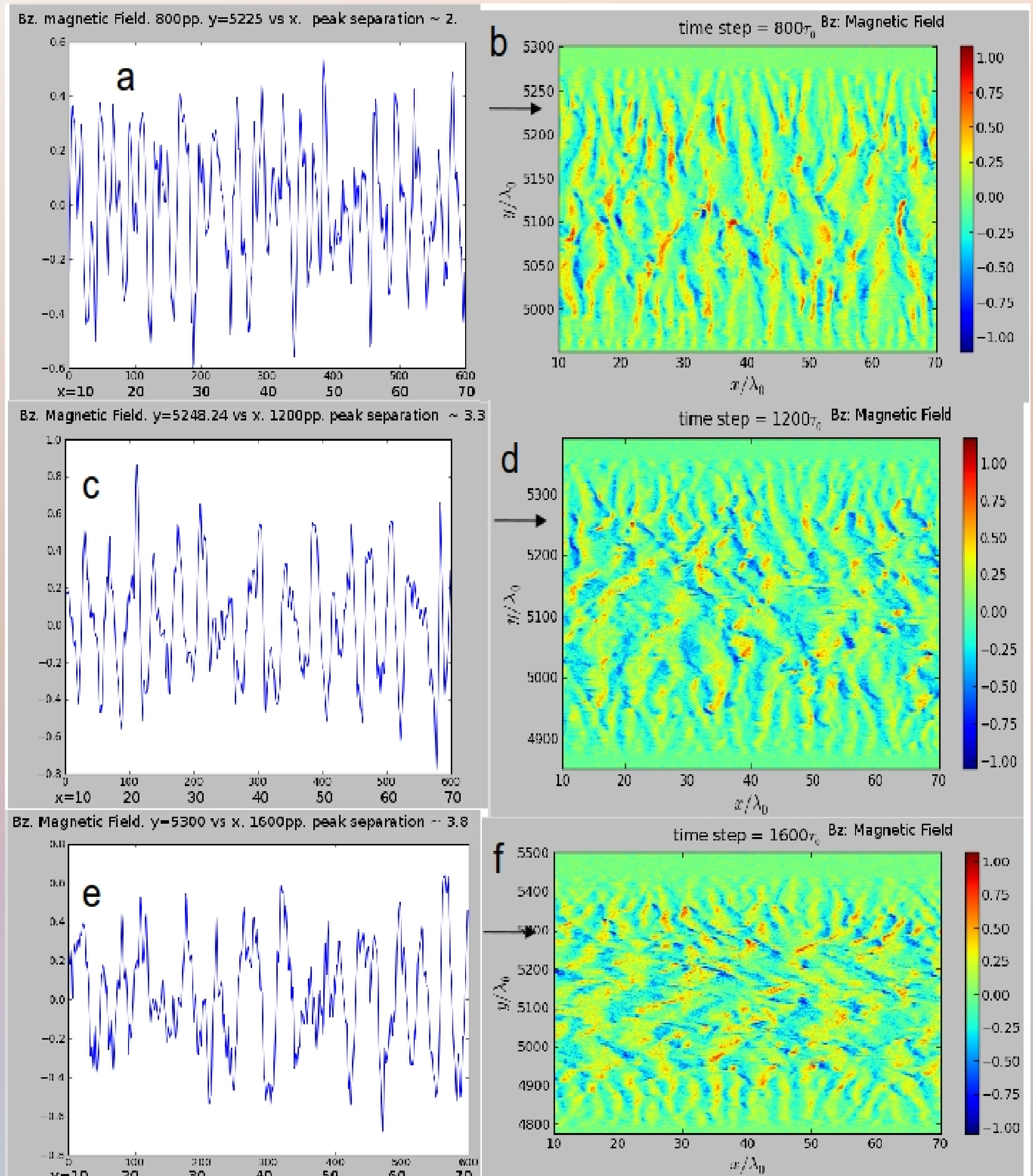

At the top, upstream from the target plasma at bottom, peak to peak separation increases in time for cuts made in the same general area.

Global Properties: Temporal Evolution of Electron Particle Density for simulation times 10, 20, 30, 40

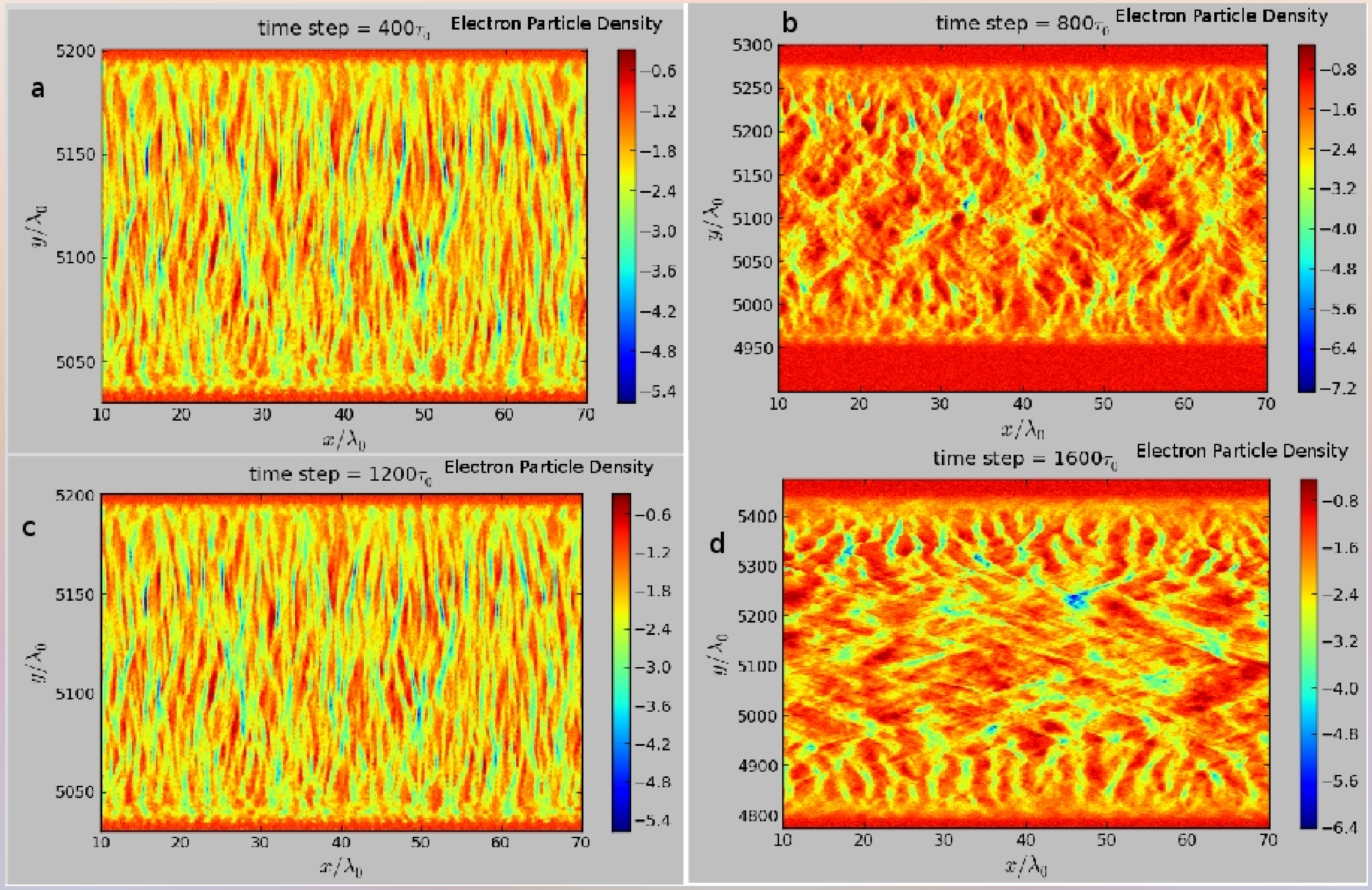

Pattern continues for Electron Particle Density

Global Properties: Evolution of Ion Particle Density time evolution for simulation times 10, 20, 30, 40

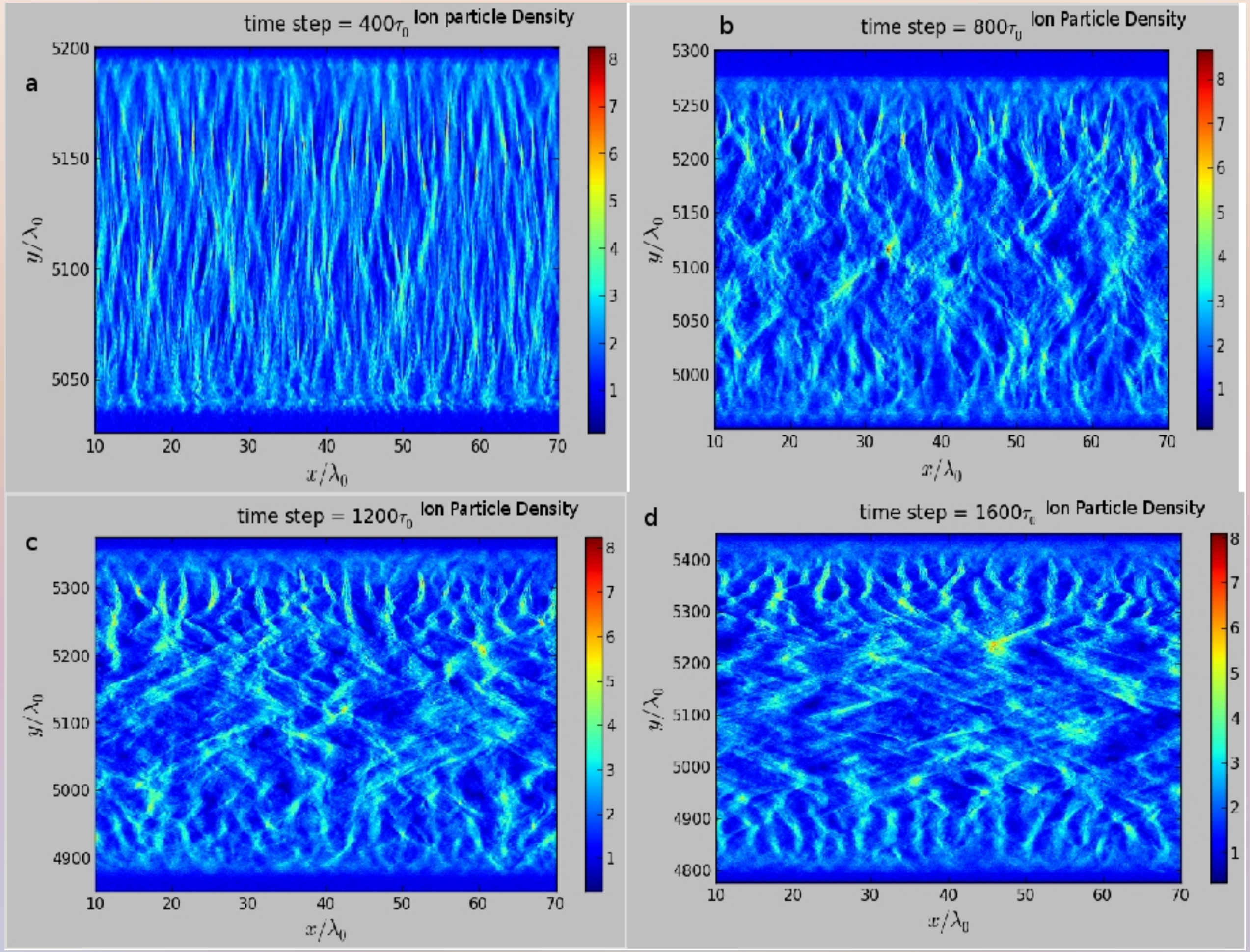

w.r.t electron particle density evolution, the ion filaments are localized inside the electron filaments with significantly higher max density

Magnetic Field z--Component Temporal Evolution for simulation times 10, 20, 30 and 40

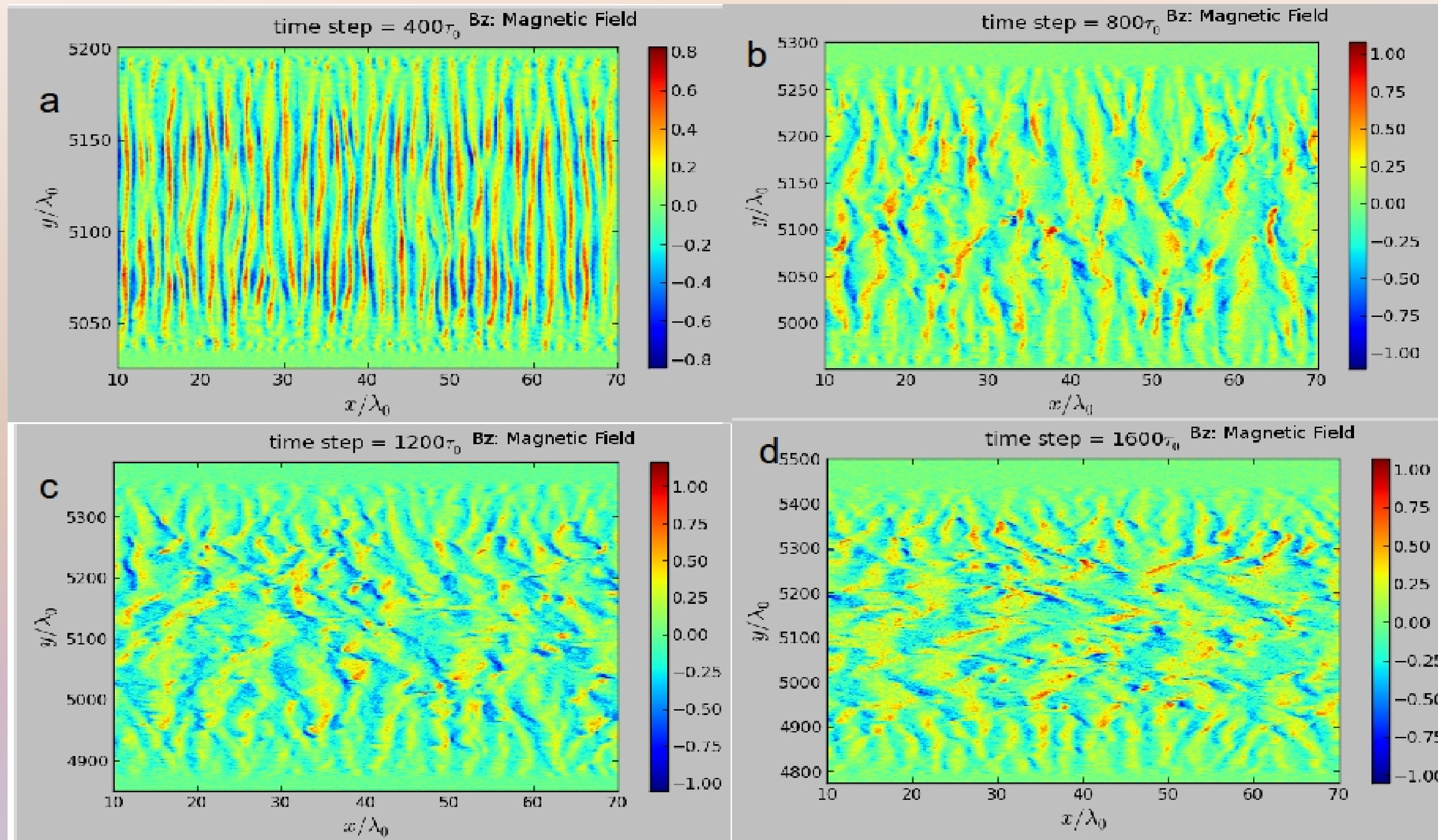

Early on, Weiblel – like filaments occur and then break up and disperse. B~ 0.8$m_e\omega_{pe}$/e; current j~0.4en_0c. The magnetic field is the result of the Weibel instability. Filament scales, position: correlate with density, energy

Bz filament row with Bz magnetic field for three simulation snapshots at simulation times 20, 30 and 40

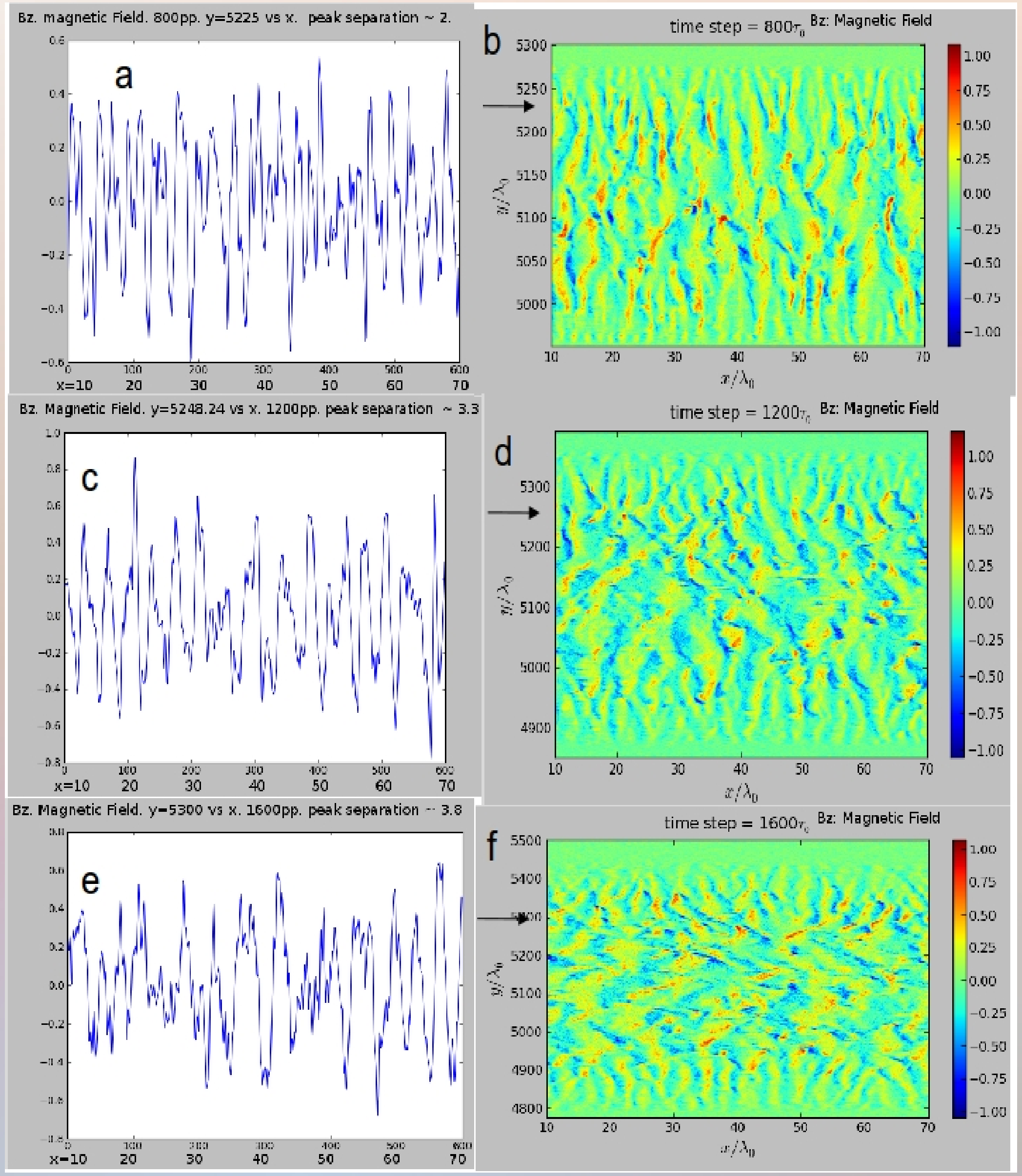

At the top, upstream from the target plasma at bottom, peak to peak separation increases in time for cuts made in the same general area.

Global Properties: Temporal Evolution of the Fields. Electric Field x--Component time evolution for simulation times 10, 20, 30, 40

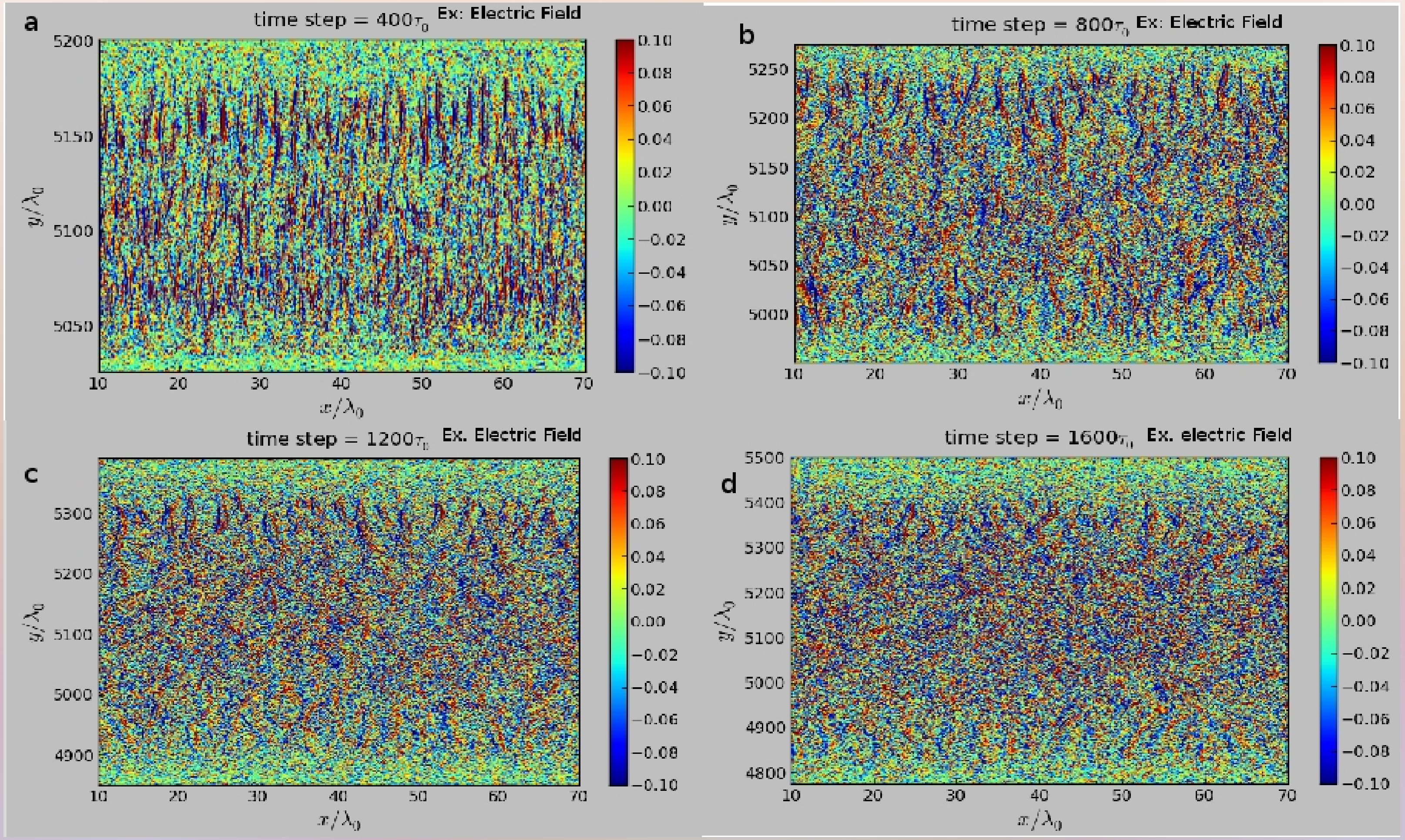

E_x : secondary effect: appears later in time w.r.t. when electron filaments were formed & the ions are driven into the electron filaments. E_x is of the order 0.1/0.6=0.16 w.r.t B_z <=> relative velocity electron/ion V_y which generate these fields

Electric Field x--Component. Three filament rows for the single simulation time 10

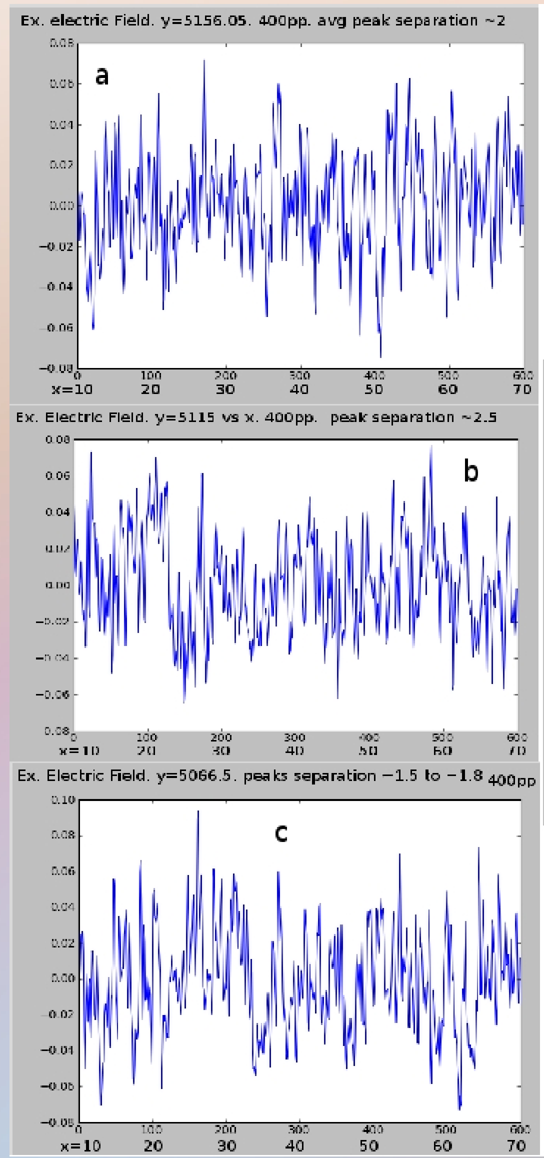

Peak to peak separation increase slightly for the middle cut

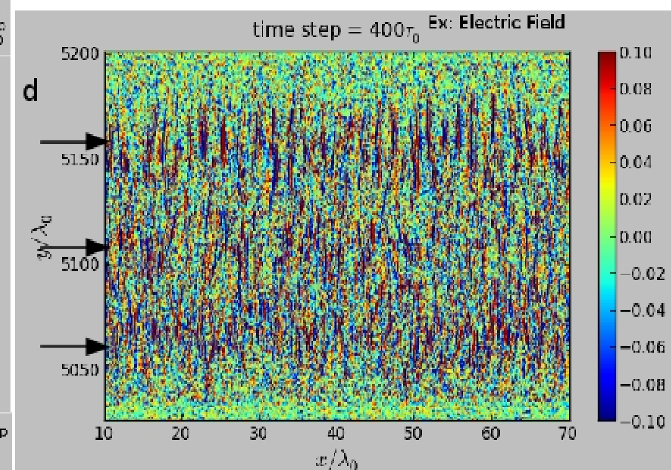

Single Filament: Electron Energy Density. Electron Energy Density Time Evolution for simulation times 10, 20, 30 and 40

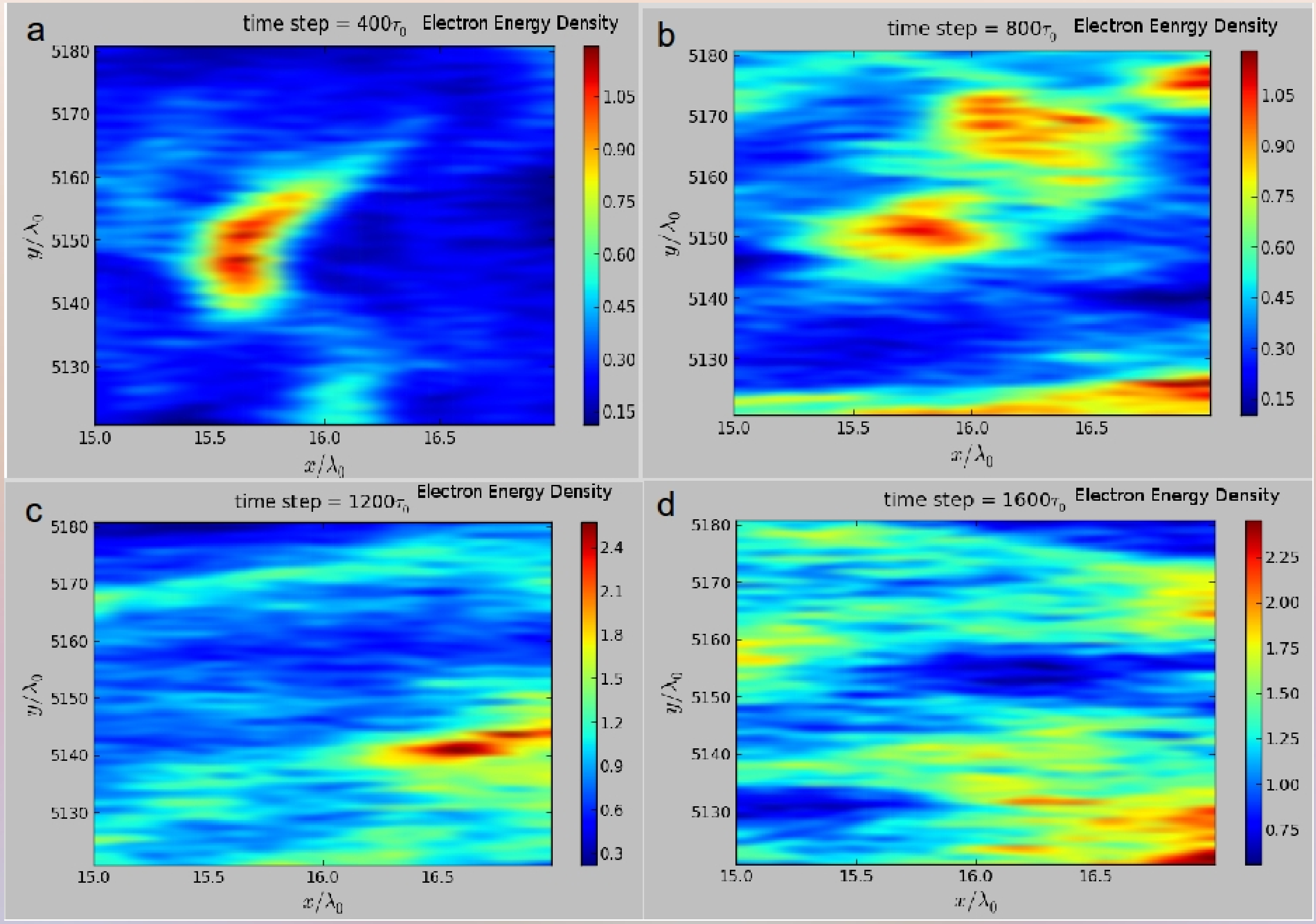

Single filaments appear later in time as a result of merging of initial small-scale filaments and that they live a relatively short time

Single Filament: Particle--Field Correlation at Simulation Time 10

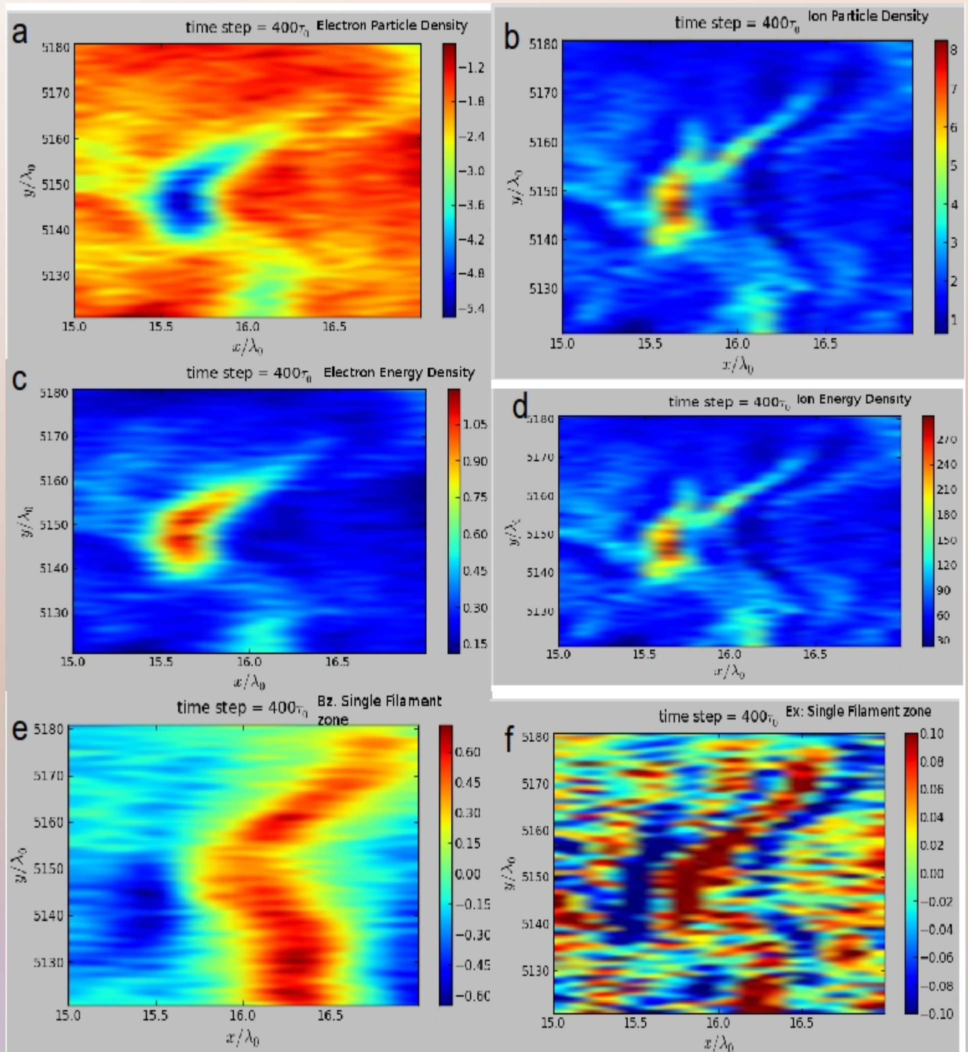

(a) and (b) electron particle density vs ion particle density: we see that the ions follow the electrons

(c) and (d) electron energy density vs ion particle density in units of $n_e = 10^{18}$. Notice energy difference. Energy Density in the units of $n_e m_e c^2$, where $m_e c^2 = 0.511$ MeV.

(e) and (f): B_z vs Field E_x for this single filament zone. Here, the Weibel instability pulls electrons into the filament speckle while the electric fields pulls ions into the filament. The magnetic field is seen shaping the filament.

Particle--Field Correlations for a zone within the overlapping region containing a single filament. Time 20. Short filament lifetime.

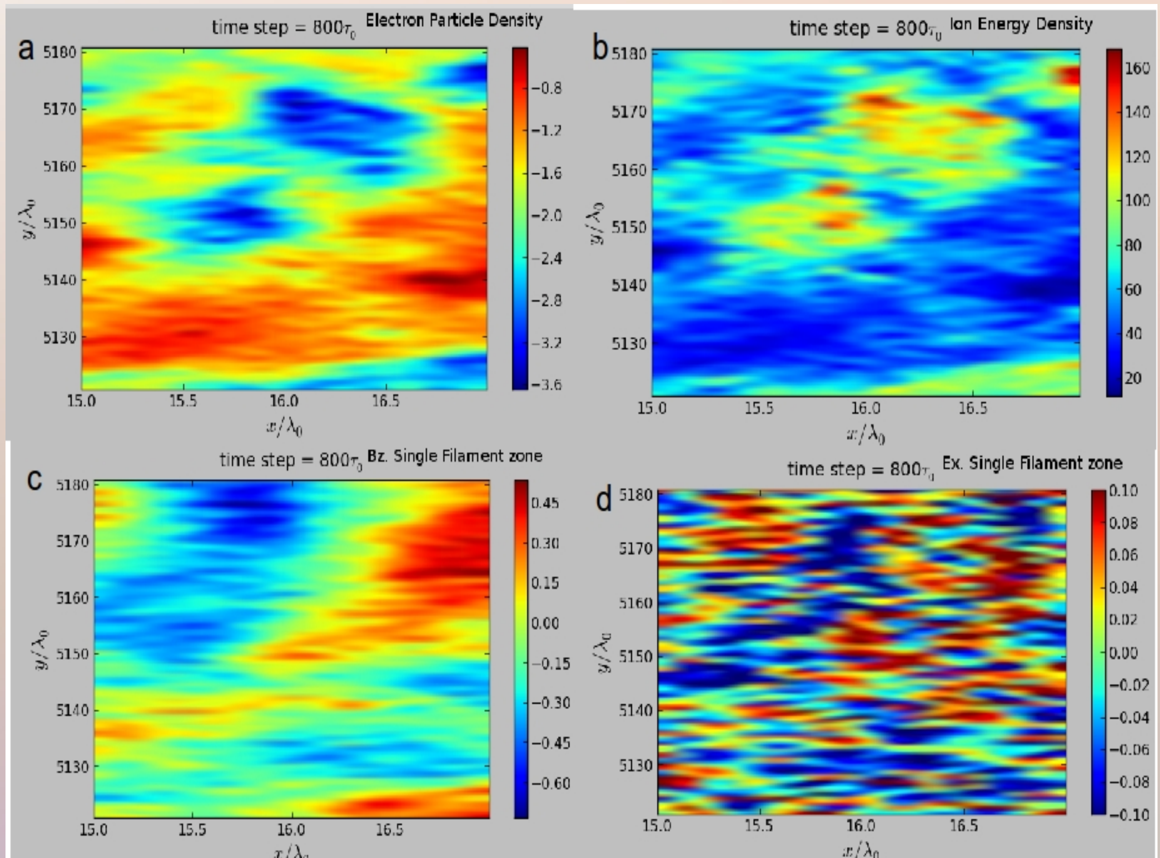

(a) and (b) time 20, electron particle density vs ion energy density. ions: follow electrons during the dispersion process (the filament residuals are seen breaking up and merging to create new filaments in (b)).

(c) and (d): B_z vs E_x in units of $m_e w_{pe} c/e$. Energy density are expressed in units of $n_e m_e c^2$, where $m_e c^2$=0.511 MeV = 511 keV. B_z and E_x are involved in breaking the filament up and dispersing the remnants through out the zone. The fields color code corresponds to the different levels of field

Single Filament: Electron Particle Density. Temporal Evolution

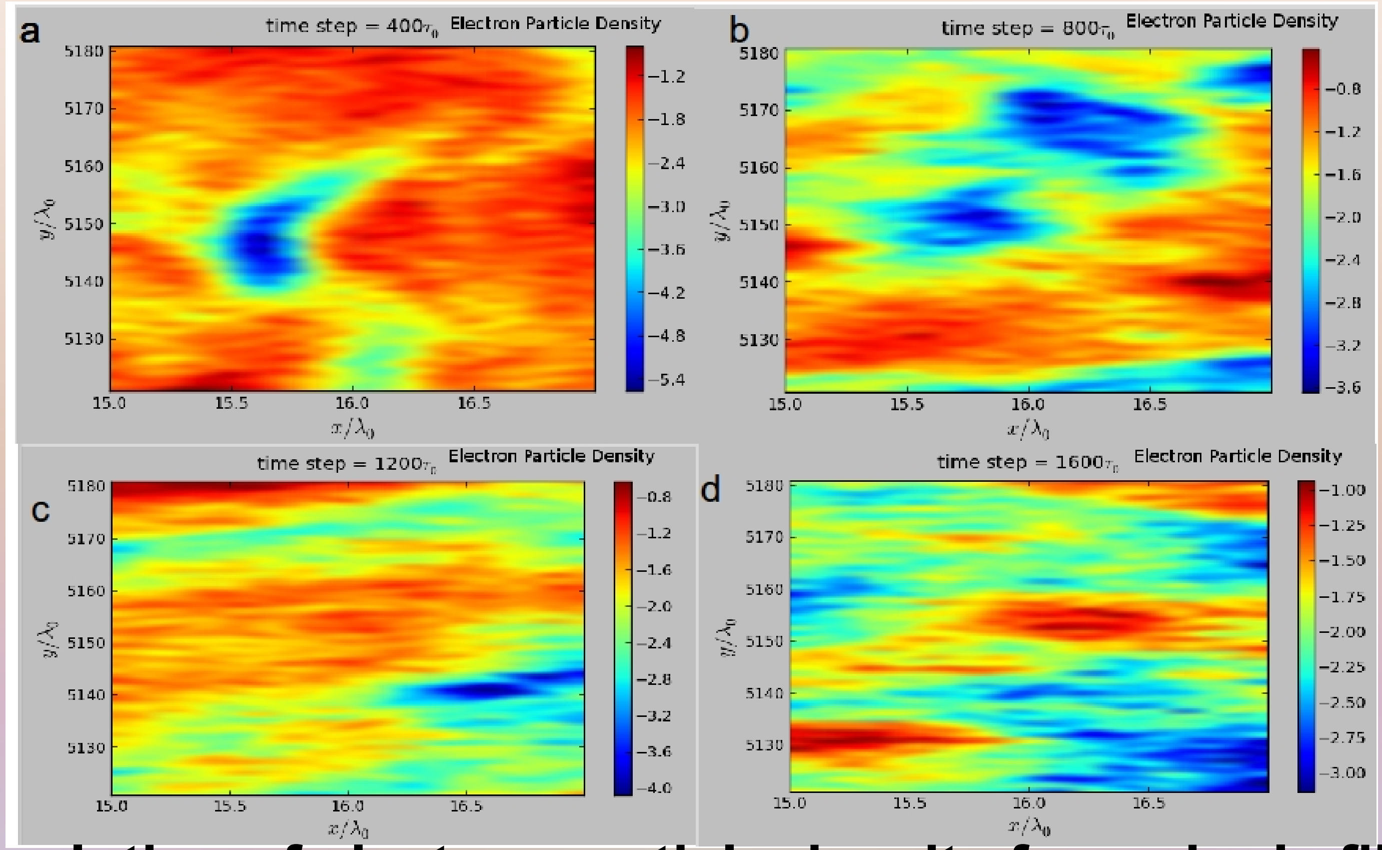

Temporal evolution of electron particle density for a single filament (a) at simulation time 10, (b) at simulation time 20, (c) at simulation time 30 and (d) at simulation time 40 inside the simulation box. Electron particle density perturbation $\delta n_e/n_0$~5—6. Electron particle Density are expressed in units of electron number density

Distribution Function over Simulation Box

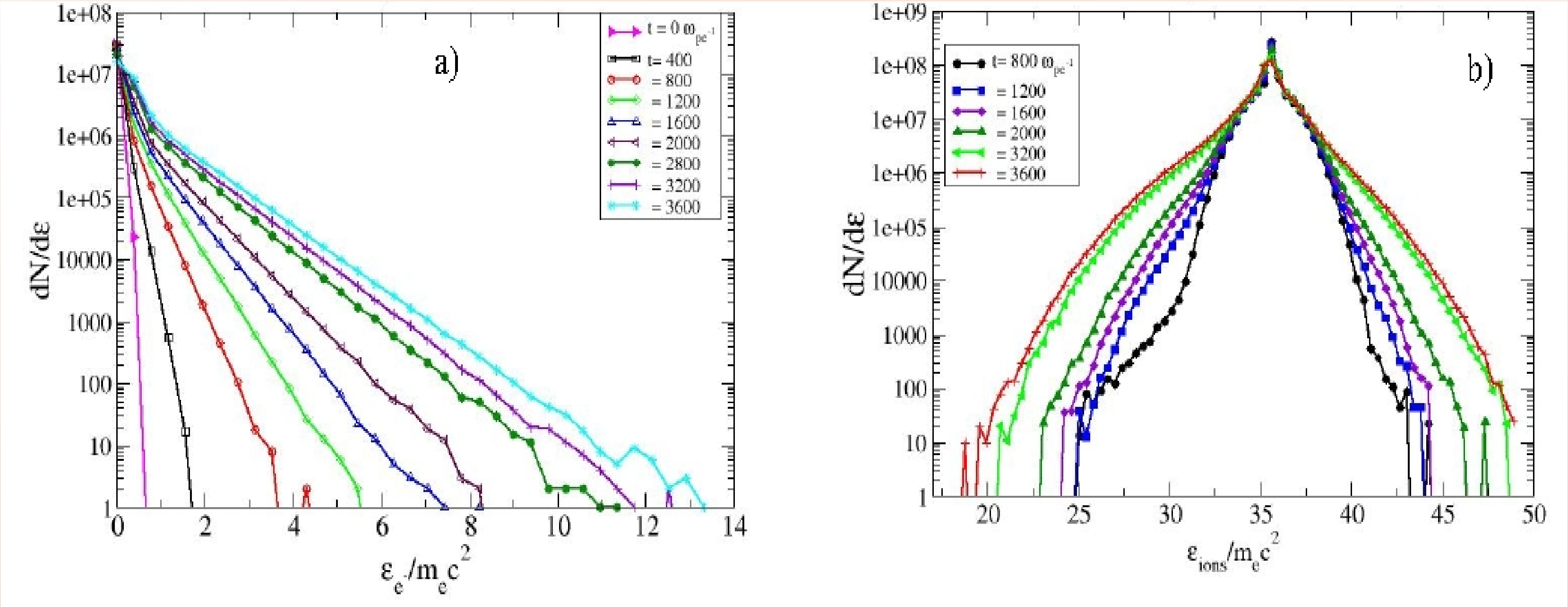

Temporal evolution of the electron (a) ion (b) distribution functions in the simulation box. (a): exponential dependence on energy: a characteristic of stochastic heating: occurs before the ion slowing down. (b) shows the kinetic energy of ions evolving with time. The color code: different time slices.

The source of the electron heating is kinetic energy of ions. The initial ion distribution corresponds to a narrow peak around the streaming energy. The electrons are gaining their energy steadily in the filaments and at time 30 they are arriving to the relativistic temperatures; However, the ion plasma heating occurs later, after the electrons. Soon: we will show this explicitly (Capdessus, 2012, in preparation)

Summary

PIC simulations: TNSA + secondary plasma target => electron heating for Counter-streaming plasmas at v~0.2c, temperature 100ev and 10 keV. Focus on initial time < 40 out of 210 total: where the electron heating is activated

Weibel—like filamentation occurs early on at time 10. New simulations with finer time Resolution will yield new insights

Ions follow electrons. Source of electron heating is the kinetic energy of ions. Ion Energy density is ~100 times electron energy density

Electron heating with associated Weibel like filamentation is the source of energy Transfer for two interpenetrating plasmas. Electron heating is a stochastic collisionless process: occurs before the ion slowing down

The average electron energy density increases and levels off for the final time. Average ion energy density decreases at the final time, indicating ion slowing down

Single filament evolution shows more global properties. Initially: electrons are pulled into the speckle by the Ampere force. Weibel instability produces electron density modulation (~5—6) in the direction perpendicular to the streaming axis with the period of the order of 2~3 electron inertia length. Filament length is ~ 100 electron inertia length, consistent with FT. Ions are accelerated transversally leading to high density ion spikes, filament merging, destruction and new filaments. The ion stream collision inside the speckles leads to strong electron heating by a factor ~ 100. Ion screening is inhibited.

Conclusions

Collisionless shocks yield new insights on phenomena as supernova, gamma ray bursts afterglows and charge particle acceleration to ultra high energies.

This type of investigation can help explain the process of their formation including conditions on how the ambient magnetic field is formed.

From our PIC simulations, shock formation is associated with early development of electron Weibel-like instabilities, subsequent electron heating and ion slowing down. The overall time of this process is long and the shock has not occurred yet.
It takes hundreds of ion plasma periods for ions to slow down and to form a shock.

Future: This type of Analysis needs to be automated. Perhaps a procedure based On Bayesian inference should be be considered. Application: since Weibel instability is resistance seen in fusion energy reactions, perhaps one could automatically determine the resistance ahead of the burn wave and eliminate it.